ARCHIVES of FOUNDRY ENGINEERING

ISSN (1897-3310)
Volume 14
Special Issue
3/2014

9 – 14

2/3

Published quarterly as the organ of the Foundry Commission of the Polish Academy of Sciences

The Model and Numerical Analysis of Hardening Phenomena for Hot-work Tool Steel

A. Bokota *, A. Kulawik, R. Szymczyk, J. Wróbel
Institute of Computer and Information Sciences, Czestochowa University of Technology,
Dąbrowskiego 73, 42-200 Częstochowa, Poland
*Corresponding author. E-mail address: bokota@icis.pcz.pl

Received 14.07.2014; accepted in revised form 22.08.2014

Abstract

In the paper the complex model of hardening of the hot-work tool steel is presented. Model of estimation of phase fractions and their kinetics is based on the continuous cooling diagram (CCT). Phase fractions which occur during the continuous heating and cooling (austenite, pearlite or bainite) are described by Johnson-Mehl-Avrami-Kolmogorov (JMAK) formula. To determine of the formed martensite the modified Koistinen-Marburger (KM) equation is used. The stresses and strains are calculated by the solution of equilibrium equations in the rate form. Model takes into account the thermal, structural, plastic strains and transformation plasticity. The thermophysical properties occurring in the constitutive relations are dependent on phase compositions and temperature. To calculate the plastic strains the Huber-Mises plasticity condition with isotopic hardening is used. Whereas to determine transformations induced plasticity the Leblond model is applied. The numerical analysis of phase compositions and residual stresses in the hot-work steel element is considered.

Keywords: Heat treatment, Hot-work tool steel W360, Phase transformation, Stresses, Thermo-elastic-plastic finite element analysis

1. Introduction

The heat treatment of hot-work tool steel is a technological process, in which thermal phenomena, phase transformations and mechanical phenomena are dominant. Models, which describe processes mentioned above, don't take into consideration the many important aspects. As a result of the complexity of phenomenon of heat treatment process, there are many mathematical and numerical difficulties in its modelling. For this reason there hasn't a model which include phenomenon accompanying heat treatment and hardening [1-4].

The correct prediction of the final properties of hardening element is possible after defining the type and the property of the nascent microstructure of the steel element in the process of heating, and then in the quenching. Recently, in many researches have been made the analysis of quenching process with using the finite element simulation technique [2,3,5-7].

In this paper the numerical model of phase transformation such as JMAK model for the diffusional transformation and modified KM model for the diffusionless transformation were employed to investigate a phase fractions during the heating and quenching process. [2,4,8].

Representing of mechanical phenomenon in process of heat treatment are mainly stress and their determinations. This values are depend on accuracy computing temperature fields and on kinetics of phase transformations in solid state. The kinetics of phase transformations has significant impact on temporary

stresses and then on residual stresses [2,5,6,9]. Numerical simulations of steel hardening process need therefore to include thermal, plastic, and structural strains and transformations induced plasticity. Inclusion of transformation plasticity has a influence on distributions and extreme values of stresses in the simulation of the hardening [2,5,10-12].

To implement this type of algorithms one usually applies the FEM, which makes it possible to take into account both nonlinearities and inhomogeneity of thermally processed material [2,6,7,13].

2. Mathematical and numerical models

The fields of temperature are determined from heat transfer equation:

$$\mathrm{div}\left(\lambda \mathrm{grad}(T)\right) - C\frac{\partial T}{\partial t} = -Q^{v},\ T = T(x_{\alpha}, t) \tag{1}$$

where $\lambda=\lambda(T)$ is the heat conductivity coefficient, $C=C(T)$ is an effective heat capacity, Q^v is intensity of internal sources in which the heat of phase transformations are taken into account, x_α are the coordinates and t is time.

Superficial heating and cooling are realised in the model by the Newton boundary condition with convection coefficient dependent on temperature [2,3,6]:

$$-\lambda\left.\frac{\partial T}{\partial n}\right|_{\Gamma} = q_n = \alpha(T)\left(T\big|_{\Gamma} - T_{\infty}\right) \tag{2}$$

where $\alpha(T)$ is the heat transfer coefficient, Γ is surface, from which the heat is taken over, T_∞ is temperature of the medium rounded.

In the model of phase transformations the continuous cooling diagram (CCT) is used (Fig. 1) [14,15]. The phase fractions, which transformed during continuous heating and cooling, austenite, pearlite or bainite are determined in model by JMAK formula. The fraction of the formed martensite is calculated using the modified KM formula [2,6,16]:

$$\begin{aligned}
&\tilde{\eta}_A(T,t) = 1 - \exp(-b(t_s,t_f)(t(T))^{n(t_s,t_f)}, \text{ heating}\\
&\eta_{BP}(T,t) = \eta_m\left(1 - \exp\left(-b(t(T))^{n}\right)\right), \text{ cooling}\\
&\eta_M(T) = \eta_m\left(1 - \exp\left(-\left((M_s - T)/(M_s - M_f)\right)^{m}\right)\right), \text{ cool.}
\end{aligned} \tag{3}$$

where $\eta_m = \eta^{\%}_{(.)}\tilde{\eta}_A$ for $\tilde{\eta}_A \geq \eta^{\%}_{(.)}$ and $\eta_m = \tilde{\eta}_A$ for $\tilde{\eta}_A < \eta^{\%}_{(.)}$, $\eta^{\%}_{(.)}$ is maximal phase fraction for established cooling rate estimated on the basis of CCT diagram, $b(t_s,t_f)$ and $n(t_s,t_f)$ are coefficients calculated assuming the initial fraction ($\eta_s(t_s)=0.01$) and the maximum value of fraction ($\eta_f(t_f)=0.99$), $\tilde{\eta}_A$ is the fraction of forming austenite after heating, m is a constant from experiment; for considered steel $m = 3.5$, the start temperature of martensite transformation amount M_s=548 K, and final temperature of transformation is equal M_f=123 K [14,16].

Latent heat, which was generated due to phase transformations, caused the increase of the temperature of the treated material. This internal heat source could be taken into account by enthalpy changes. Therefore, the following enthalpy changes for the diffusional and diffusionless transformations were used ([J/m^3]) [2,4,6,16]:

$$\Delta H_B = 314\times10^6,\ \Delta H_M = 630\times10^6,\ \Delta H_P = 800\times10^6 \tag{4}$$

where ΔH_B, ΔH_M and ΔH_P indicate the enthalpy changes during austenite-bainite, austenite-martensite and austenite-pearlite transformations, respectively.

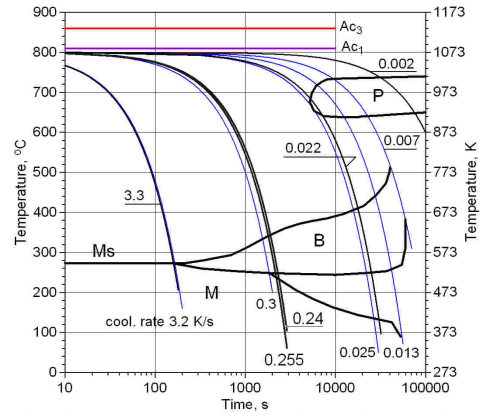

Fig. 1. The Time-Temperature-Transformation graph (CCT) for tools steel W360 [8,9]

Heat of phase transformations is taken account by the volumetric heat source in the conductivity equation (1) and is calculated with the formula [6,16]

$$Q^{v} = \dot{Q}^{ph} = \sum_k \dot{Q}_k^{\eta_k} = \sum_k H_k^{\eta_k}\dot{\eta}_k,\ k = 2...5 \tag{5}$$

where H_k is volumetric heat (enthalpy) k- phase transformations, $\dot{\eta}_k$ is the rate of change k- phase fraction.

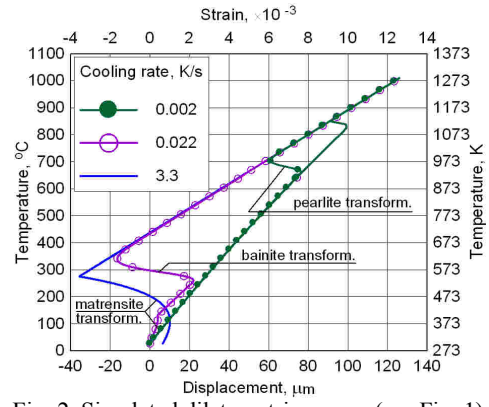

Fig. 2. Simulated dilatometric curves (see Fig. 1)

For the examined steel, values of thermal expansion coefficients and isotropic structural strains of each micro-constituents were determined. They equal: 22, 12.5, 12.5 and 14.7 ($\times 10^{-6}$) [1/K] and 1.8, 6.0, 8.5 and 2.53 ($\times 10^{-3}$) for austenite, bainite, martensite and pearlite respectively [2,6,16].

The example of the results of the simulations comparisons are presented the figure 2, the kinetic of transformations established cooling rate (the average cooling rate in the range of 800-500°C [14]) are presented on the figure 3.

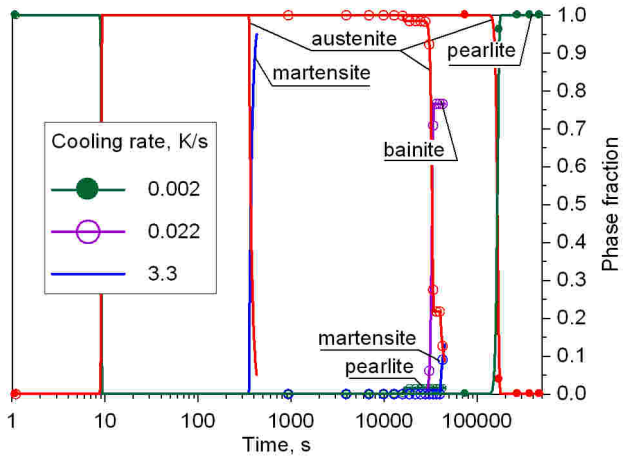

Fig. 3. The kinetic of transformations for established cooling rate

The simulated dilatometric curves were obtained by solving the increment of the isotropic strain ($\boldsymbol{\varepsilon}^{Tph}$) in the processes of heating and cooling [6,16].

Coefficient of thermal expansion of the pearlite structure for considered steel is assumed as dependent on temperature (see Fig. 2), approximate this coefficient by square function [16]:

$$\alpha_P(T) = 5.556\times 10^{-13} T^2 + 3.419\times 10^{-9} T + 9.747\cdot 10^{-6} \tag{6}$$

The equilibrium equation and constitutive relations are used in rate form [2,16], i.e.:

$$\operatorname{div}\dot{\boldsymbol{\sigma}}(x_\alpha, t) = \mathbf{0},\ \dot{\boldsymbol{\sigma}} = \dot{\boldsymbol{\sigma}}^T,\ \dot{\boldsymbol{\sigma}} = \mathbf{D}\circ\dot{\boldsymbol{\varepsilon}}^{\mathrm{e}} + \dot{\mathbf{D}}\circ\boldsymbol{\varepsilon}^{\mathrm{e}} \tag{7}$$

where $\boldsymbol{\sigma}=\boldsymbol{\sigma}(\sigma_{\alpha\beta})$ is stress tensor, $\mathbf{D}=\mathbf{D}(\nu,E)$ is the tensor of material constants (isotropic materials), ν is Poisson ratio, $E=E(T)$ is the Young's modulus, however $\boldsymbol{\varepsilon}^e$ is tensor elastic strains.

The equation (7) is completed by initial conditions

$$\boldsymbol{\sigma}(x_\alpha, t_0) = \mathbf{0},\quad \boldsymbol{\varepsilon}^{\mathrm{e}}(x_\alpha, t_0) = \mathbf{0} \tag{8}$$

and boundary conditions which provide external statically determinate.

Total strains in the around considered points are result of the sum:

$$\boldsymbol{\varepsilon} = \boldsymbol{\varepsilon}^e + \boldsymbol{\varepsilon}^{Tph} + \boldsymbol{\varepsilon}^{tp} + \boldsymbol{\varepsilon}^p \tag{9}$$

where $\boldsymbol{\varepsilon}^{Tph}$ are isotope of temperature and structural strains, $\boldsymbol{\varepsilon}^{tp}$ are transformations plasticity, and $\boldsymbol{\varepsilon}^p$ are plastic strains.

For the Huber-Misses plasticity condition the flow function (f) have the form [2,5,7,16]:

$$f = \sigma_{ef} - Y\left(T, \sum Y_0^k(T)\eta_k, \varepsilon_{ef}^{\mathrm{p}}\right) = 0 \tag{10}$$

where σ_{ef} is effective stress, $\varepsilon_{ef}^{\mathrm{p}}$ is effective plastic strain, Y is a plasticized stress of material on the phase fraction (η) in temperature (T) and effective strain (ε_{ef}^{p}):

$$Y\left(T, \sum Y_0^k(T)\eta_k, \varepsilon_{ef}^{\mathrm{p}}\right) = Y_0\left(\sum Y_0^k(T)\eta_k\right) + Y_H\left(T, \varepsilon_{ef}^{\mathrm{p}}\right) \tag{11}$$

$Y_0 = Y_0\left(\sum Y_0^k(T)\eta_k\right)$ is a yield points of material dependent on the temperature and the phase fraction, however $Y_H = Y_H\left(T, \varepsilon_{ef}^{p}\right)$ is a surplus of the stress resulting from the material hardening.

Using the Leblond model, completed by decreasing functions $(1-\eta)$ which has been proposed by the authors of the work [2,5,11,12], transformations plasticity are calculated as following:

$$\dot{\boldsymbol{\varepsilon}}^{\mathrm{tp}} = \begin{cases} 0, \text{ dla } \eta_k \le 0.03, \\ -3\sum_{k=2}^{k=5}(1-\eta_k)\varepsilon_{1k}^{ph}\dfrac{\mathbf{S}}{Y_1}\ln(\eta_k)\dot{\eta}_k, \text{ dla } \eta_k \ge 0.03 \end{cases} \tag{12}$$

where $3\varepsilon_{1i}^{ph}$ are volumetric structural strains when the material is transformed from the initial phase „1" into the k-phase, Y_1 is a actual yield points of phase output (in cooling process is austenite).

The equations (7) are solved by using the FEM [13,16]. The system of equations used for numerical calculation is:

$$[\mathbf{K}]\{\dot{\mathbf{U}}\} = \left(\{\dot{\mathbf{R}}\} + \{\dot{\mathbf{t}}^{Tph}\} - \{\dot{\mathbf{t}}^{e}\}\right) + \{\dot{\mathbf{t}}^{ptp}\} \tag{13}$$

where $\mathbf{K}$ is the element stiffness matrix, $\mathbf{U}$ is the vector of nodal displacement, $\mathbf{R}$ is the vector of nodal forces resulting from the boundary load and the inertial forces load, $\mathbf{t}^{Tph}$ is the vector of nodal forces resulting from thermal strains and structural strains, $\mathbf{t}^{e}$ is the vector of nodal forces resulting from the value change of Young's modulus dependent on the temperature, $\mathbf{t}^{ptp}$ is the vector of nodal forces resulting from plastic strains and transformation plasticity.

The final displacements, strains and stress are resulting integration with respect to time, from initial $t=t_0$ (see (8)) to actual time t, i.e.

$$\begin{aligned} \mathbf{U}(x_\alpha, t) &= \int_{t_0}^{t} \dot{\mathbf{U}}(x_\alpha, \tau)d\tau \\ \boldsymbol{\varepsilon}(x_\alpha, t) &= \int_{t_0}^{t} \dot{\boldsymbol{\varepsilon}}(x_\alpha, \tau)d\tau,\ \boldsymbol{\sigma}(x_\alpha, t) = \int_{t_0}^{t} \dot{\boldsymbol{\sigma}}(x_\alpha, \tau)d\tau \end{aligned} \tag{14}$$

The rate vectors of loads in the brackets in (13) are calculated only once in the increment of the load, whereas the vector $\mathbf{t}^{ptp}$ is modified in the iterative process [12]. In the iterative process of evaluation of plastic strains, the modified Newton-Raphson algorithm is used [13,17].

3. Example of numerical calculations

To hardening simulation the axisymmetric element with dimensions ϕ50×100 mm was used (Fig. 4). Numerical simulations of hardening of the elements made of the hot-work tool steel W360 were performed.

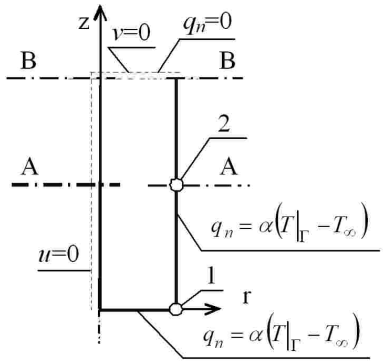

Fig. 4. The scheme of the system and boundary conditions

It was assumed that hardened element has the temperature equal 300 K and the output structure is pearlite (divorced pearlite). The element was heating in the fluidized bed with temperature 1600 K. The thermophysical coefficients C and λ were assumed as constants: 5.34×10^6 J/(m^{3}K) and 32 W/(mK). These are the average values calculated on the basis of the data in the work [14]. The heat transfer coefficient of the fluidized bed assumed constant (independent of temperature) and equal 2400 W/(m^{2}K). On the front surface of heated element the heat transfer coefficient had the value 1200 W/(m^{2}K). By using these value of coefficient the difficult (worse) flow around a fluidized bed on the front of surface of element was taken into account [18]. The simulation of heating was continuing to obtain the maximum temperature 1350 K in surroundings of point 1 (Fig. 4). The temperatures Ac_1 and Ac_3 in the phase transformations of heating (input structure - austenite) were equal 1033 and 1133 K appropriately (Fig. 1) [14].

The obtained temperature distribution and austenite zone after finish of heating are presented in figure 5.

The cooling was modelled with the Newton condition and the extreme of heat transfer coefficient assumed equal 20 W/(m^{2}K) (cooling in the air [14]). The temperature of the cooling medium equalled T_∞=300 K.

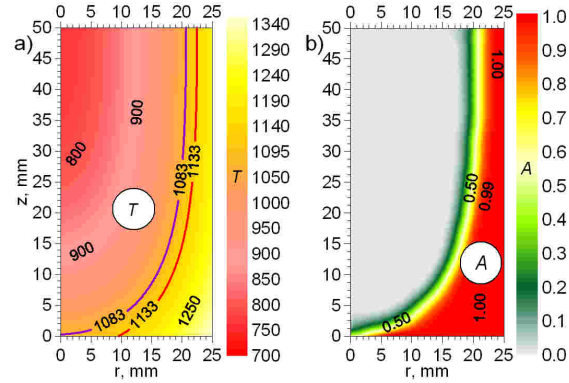

Fig. 5. Distributions of temperature a) and austenite b) after heating. Isolines with values 1033 and 1133 K, are the temperature of Ac_1 and Ac_3 appropriately

Hardened zones in the cross sections of the element are presented in figures 6 and 7. Distributions of the simulated fractions in the cross-section A-A (Fig. 4) after hardening are presented in figure 8.

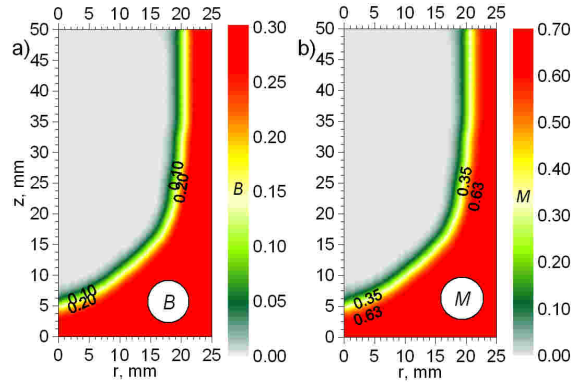

Fig. 6. Distributions of bainite a) and martensite b) after cooling

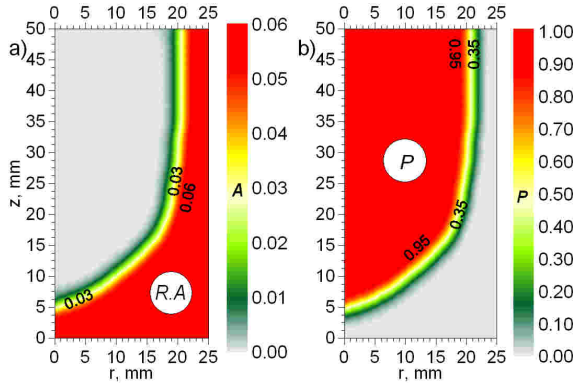

Fig. 7. Distributions of retained austenite a) and pearlite b) after cooling

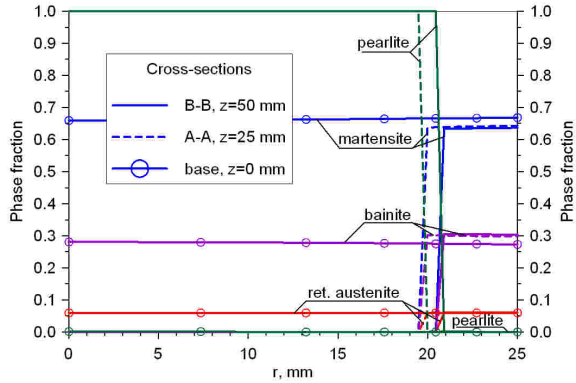

Fig. 8. Hardened zones in the cross sections (Fig. 4)

Young's and tangential modulus (E and E^t) were dependent on temperature, whereas the yields stress (Y_0) was dependent on temperature and phase composition. Assumed, that Young's and tangential modulus are equal 2×10^5 and 4×10^3 MPa ($E^t=0.05E$), yield points 150, 500, 1000 and 300 MPa for austenite, bainite, martensite and pearlite, respectively, in the temperature 300 K. In the temperature of solidus Young's modulus and tangential modulus equalled 100 and 10 MPa, respectively, whereas yield points equalled 5 MPa. These values were approximated with the use of square functions using the following assumptions based on the work [5,6,16].

Obtained from simulations residual stresses distributions after hardening are presented in figures 9-12.

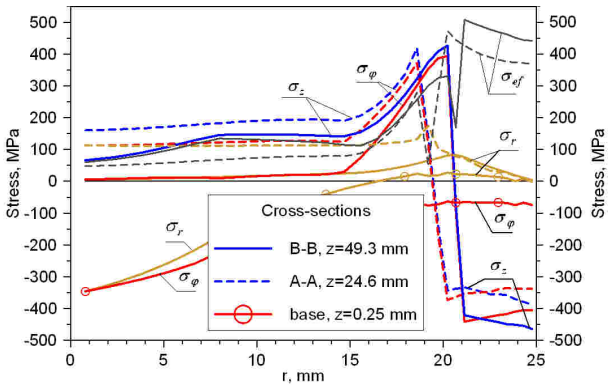

Fig. 9. Residual stresses in the cross sections (Fig. 4)

4. Conclusions

The results of the phase transformations model are satisfactory and confirm the correctness of the designed model of phase transformations for the hot-work tool steel (Figs 6 and 7). On the basis of simulated dilatometric curves can see that the considered steel is hardened very easy. To obtain the bainite-martensite structure the cooling rate can't be greater than 3.2 K/s (see Figs 1,2 and 3). Therefore the cooling in the air was applied and the cooling rate was equal 0.24 K/s in the point 2 (Fig. 4). In the point 1 the cooling rate was a bit greater and had a value 0.255 K/s (see Fig. 1).

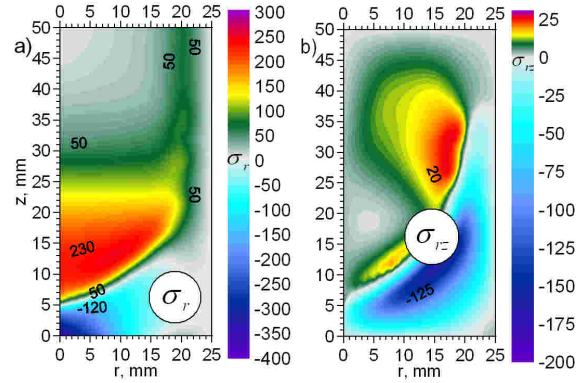

Fig. 10. Residual stresses: radial a) and shear b)

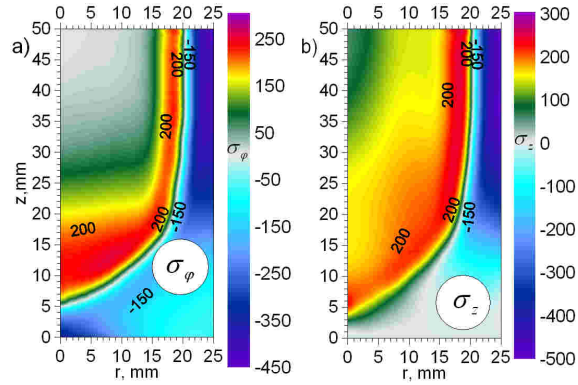

Fig. 11. Residual stresses: circumferential a) and axial b)

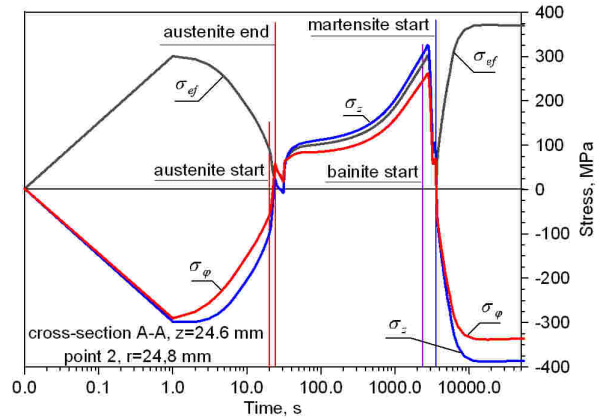

Fig. 12. Stresses according to the time (point 2, Fig. 4)

The stresses distributions after such hardening are advantageous. The regular distributions of the stresses are obtained. The extreme values of these stresses are acceptable. The deposition of negative circumferential and axial stresses (the most meaningful stresses) is superficial (Figs 9-11), and their extreme values are lower when these stresses are taken into account. The adverse is the distribution of the shear stresses (Fig. 10b). Such stresses can be a cause of internal cracks in the cooling process.

It can be claimed that in the numerical simulation of such hardening the fact that transformation plasticity is included in the model of mechanical phenomena brings about the changes in

obtained results [10,11,16]. The phase transformations significantly effect on the changes of the temporary stresses (see Fig. 12) and in consequence on the residual stresses after hardening of the element considered.

References

[1] Kang, S.H. & Im, Y.T. (2007). Thermo-elesto-plastic finite element analysis of quenching process of carbon steel. *Intenational Journal of Mechanical Sciences*. 49. 13-16.

[2] Kang, S.H. & Im, Y.T. (2007). Three-dimensional thermo-elestic-plastic finite element modeling of quenching process of plain carbon steel in couole with phase transformation. *Journal of Materials Processing Technology*. 192-193. 381-390.

[3] Kulawik, A. & Bokota, A. (2011). Modelling of heat treatment of steel with the movement of coolant *Archives of Metallurgy and Materials*. 56(2). 345-357.

[4] Ju, D.Y., Zhang, W.M. & Zhang, Y. (2006). Modeling and experimental verification of martensitic transformation plastic behavior in carbon steel for quenching process, *Materials Science and Engineering* A. 438-440, 246-250.

[5] Coret, M. & Combescure, A. (2002). A mesomodel for the numerical simulation of the multiphasic behavior of materials under anisothermal loading (application to two low-carbon steels). *International Journal of Mechanical Sciences*. 44. 1947-1963.

[6] Bokota, A. & Kulawik, A. (2007). Model and numerical analysis of hardening process phenomena for medium-carbon steel. *Archives of Metallurgy and Materials*. 52(2). 337-346.

[7] Huiping, L., Guoqun, Z., Shanting, N. & Chuanzhen, H. (2007). FEM simulation of quenching process and experimental verification of of simulation results. *Material Science and Engineering* A. 452-453, 705-714.

[8] Oliveira, W.P, Savi, M.A., Pacheco, P.M.C.L. & Souza, L.F.G. (2010). Thermomechanical analysis of steel cylinders with diffusional and non-diffusional phase transformations. *Mechanics of Materials*. 42, 31-43.

[9] Silva, E.P., Pacheco, P.M.C.L. & Savi, M.A. (2004). On the thermo-mechanical coupling in austenite-martensite phase transformation related to the quenching process. *International Journal of Solids and Structures*. 41, 1139-1155.

[10] Serejzadeh, S. (2004). Modeling of temperature history and phase transformation during cooling of steel. *Journal of Processing Technology*. 146. 311-317.

[11] Taleb, L. & Sidoroff, F. (2003). A micromechanical modelling of the Greenwood-Johnson mechanism in transformation induced plasticity. *International Journal of Plasticity*. 19. 1821-1842.

[12] Cherkaoui, M., Berveiller, M. & Sabar, H. (1998). Micromechanical modeling of martensitic transformation induced plasticity (TRIP) in austenitic single crystals. *International Journal of Plasticity*. 14(7). 597-626.

[13] Zienkiewicz, O.C. Taylor, R.L. (2000). *The finite element method*. vol. 1,2,3. Butterworth-Heinemann, Fifth edition.

[14] Warmarbeitsstahl Hot Work Tool Steel, BOHLER W360, Iso Bloc, www.bohler-edelstahl.com.

[15] Orlich, J, Rose, A., Wiest, P. (1973). *Atlas zur Wärmebehandlung von Stähle*, III Zeit Temperatur Autenitisierung Schaubilder, Verlag Stahleisen MBH, Düsseldorf.

[16] Bokota, A. & Domański, T. (2007). Numerical analysis of thermo-mechanical phenomena of hardening process of elements made of carbon steel C80U. *Archives of Metallurgy and Materials*. 52(2), 277-288.

[17] Caddemi, S. & Martin, J.B. (1991). Convergence of the Newton-Raphson algorithm in elastic-plastic incremental analysis. *Int. J. Numer. Meth. Eng*. 31. 177-191.

[18] Jasiński, J. (2003). *Influence of fluidized bed on diffusional processes of saturation of steel surface layer*. Częstochowa: Inżynieria Materiałowa Nr 6, Wydawnictwo WIPMiFS, (in Polish).